THE JOURNAL OF PHYSICAL CHEMISTRY C

Article

pubs.acs.org/JPCC

Double Hydrophilic Block Copolymer Templated Au Nanoparticles with Enhanced Catalytic Activity toward Nitroarene Reduction

Eunyong Seo,[†] Jesi Kim,[‡] Yunjeong Hong,[†,§] Yung Sam Kim,[†] Daeyeon Lee,[∥] and Byeong-Su Kim*[,†]

[†]Interdisciplinary School of Green Energy and School of NanoBioscience and Chemical Engineering, Ulsan National Institute of Science and Technology (UNIST), Ulsan 689-798, Korea

[‡]Department of Bioengineering, University of Pennsylvania, Philadelphia, Pennsylvania 19104, United States

[§]Division of Applied Biology and Chemistry, College of Agriculture and Life Sciences, Kyungpook National University, Daegu 700-412, Korea

[∥]Department of Chemical and Biomolecular Engineering, University of Pennsylvania, Philadelphia, Pennsylvania 19104, United States

Supporting Information

ABSTRACT: We present a facile method for synthesizing water-dispersible gold nanoparticles (Au NPs) using a double hydrophilic block copolymer (DHBC), poly(ethylene oxide)-*block*-poly(acrylic acid) (PEO-*b*-PAA), as a template and demonstrate their application in the reduction of nitroarenes. Selective coordinative interactions between a gold precursor and the PAA block of the DHBC lead to the formation of micelles, which are subsequently transformed into Au NPs with an average diameter of 10 nm using a reducing agent. The DHBC-templated Au NPs (Au@DHBC NPs) remain stable in water for several months without any noticeable aggregation. Furthermore, Au@DHBC NPs are found to be highly effective in catalyzing the reduction of a series of nitroarenes. Remarkably, the turnover frequency in the case of 4-nitrophenol using Au@DHBP NPs reaches 800 h^{-1}, outperforming previously reported Au NP-based catalytic systems. We believe the enhanced catalytic activity is due to the DHBC shell around Au NPs, which templates the formation of spherical Au NPs and, more importantly, provides the confined interior for the enhanced catalytic activity in nitroarene reduction. Considering the wide potential application of DHBC as a template for the synthesis of novel metal NPs, we anticipate that the approach presented in this study will offer a new means to create a variety of water-stable catalytic nanomaterials in various fields of green chemistry.

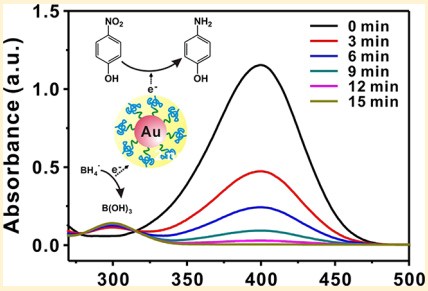

INTRODUCTION

The development of metal nanostructures has been intensively pursued over several decades for their fundamental scientific interests and technological importance in various applications.[1−5] Among noble metals, gold nanoparticles (Au NPs) have been the subject of intense investigation due to their broad applicability in biomedicine, catalysis, and biosensing. Numerous approaches to prepare Au NPs in various sizes and morphologies have been reported including citrate reduction, Brust's two-phase method, the seed growth method, thermolysis of metal precursors, and template synthesis with micelles and surfactants.[6−14]

In many of these approaches, control over the particle size and morphology was achieved by either using templating materials or capping agents during the growth of NPs. For example, small organic molecules or polymers are widely used as soft templates to form stable Au nanostructures without the aggregation of NPs. Murphy and co-workers reported that spherical Au NPs were successfully synthesized using citric acid as both capping and reducing agents. The size of as-prepared Au NPs using citric acid can even be tuned further by the seed growth method.[10,15,16] Block copolymers have recently emerged as versatile templates for synthesizing inorganic NPs because they allow for control over the size and shape of NPs and also direct the spatial patterning of NPs on the surface owing to their self-assembly capability. Toward that end, most block copolymer self-assembly approaches rely on the use of entirely hydrophobic or amphiphilic block copolymers, inevitably necessitating the use of organic solvents for synthesis and subsequent utilization. Considering that a number of applications such as wastewater treatment require the dispersion of heterogeneous catalysts in aqueous solutions and that water is by far the most environmentally friendly medium, it is crucial to develop polymer templates that will enable synthesis and stabilization of NPs in aqueous media.

In this context, double hydrophilic block copolymers (DHBCs), which consist of two chemically distinct hydrophilic segments, offer a unique alternative to the existing methods. The synthesis of metal NPs using DHBCs presents a straightforward and versatile method to produce metal nanostructures under mild aqueous conditions without the use of organic solvents or thermal treatment.[17,18] From an

Received: March 19, 2013
Revised: April 29, 2013
Published: May 13, 2013

Scheme 1. Schematic Illustration of the Synthesis of Au@DHBC NP through the Coordinative Bonding between the Au Precursor and a Double Hydrophilic Block Copolymer (DHBC) (PEO-*b*-PAA) as a Soft Template

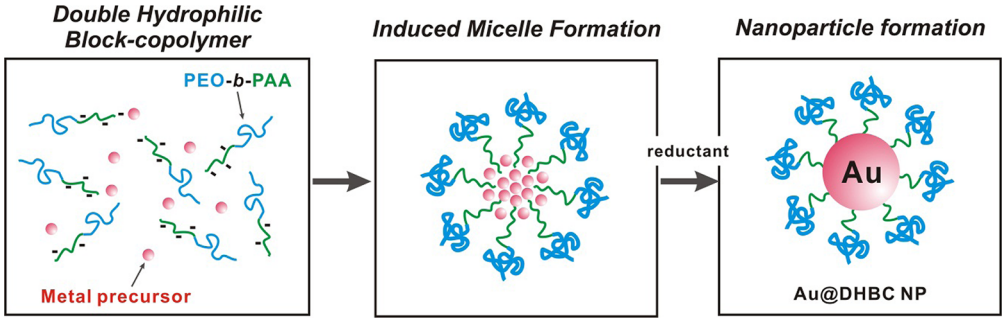

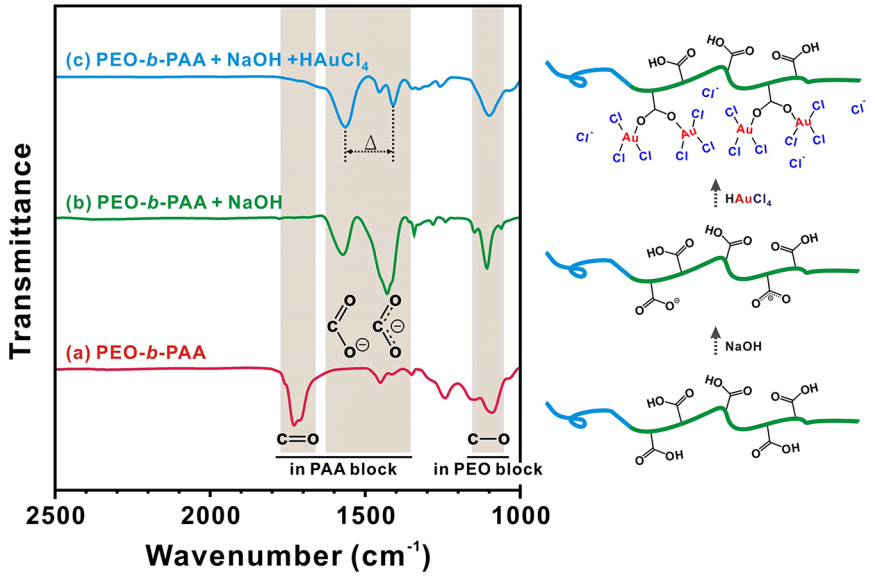

Figure 1. FT-IR spectra of (a) PEO-*b*-PAA, (b) PEO-*b*-PAA with NaOH, and (c) PEO-*b*-PAA with NaOH and Au precursor. The schematic description of the coordinative bond formation between the Au precursor and carboxylate group is displayed in the right panel.

environmental point of view, water provides numerous advantages over organic solvents as a reaction medium with its fast reaction rate, high yield, and nontoxicity.

Herein, we report the synthesis of Au NPs using a DHBC as a soft template to produce NPs with a superior aqueous stability and investigate their potential as catalysts for the reduction of a series of nitroarenes in aqueous solutions. Specifically, the DHBC, poly(ethylene oxide)-*block*-poly(acrylic acid) (PEO-*b*-PAA), is employed to form a micelle upon the addition of a gold precursor, $HAuCl_4{\cdot}3H_2O$, which is subsequently converted to Au NPs with the addition of a reducing agent. Au NPs with a proper size distribution are subsequently prepared by a simple centrifugation process. Furthermore, we find that Au@DHBC NP is a highly effective catalyst in the reduction of a series of nitroarenes. Remarkably, it is shown that the turnover frequency (TOF) reaches 800 h^{-1} in 4-nitrophenol reduction using the Au@DHBC NP catalyst. This DHBC-based method provides a simple synthetic procedure that produces hybrid Au NPs with outstanding performance in catalytic reactions. Because the self-assembly process (i.e., micellization) is driven by the simple coordinative bonding between the Au precursor and the carboxylate group of the PAA block, we anticipate that this DHBC-based method will provide a facile and general means in the synthesis of other NPs for a variety of applications.

EXPERIMENTAL METHODS

Materials and Chemicals. Gold(III) chloride trihydrate ($HAuCl_4{\cdot}3H_2O$), hydrazine (NH_2NH_2), 4-nitroarenes, and sodium borohydride were purchased from Aldrich and used without further purification. A double hydrophilic block copolymer of PEO(5000)-*b*-PAA(6700) was purchased from Polymer Source, Inc.

Synthesis of Au@DHBC NPs. The gold nanoparticles with a double hydrophilic block copolymer shell were prepared according to the following protocols. First, the double hydrophilic block copolymer PEO(5000)-*b*-PAA(6700) (25.12 mg, 0.20 mmol of carboxylic acid groups) was dissolved under vigorous stirring in 50.0 mL of deionized water, followed by adding 0.1 mL of 4.0 M NaOH (0.40 mmol, 2 equiv to carboxylic acid groups in PAA block). To this solution mixture, $HAuCl_4{\cdot}3H_2O$ (26.2 mg, 0.067 mmol) was mixed. Subsequently, 0.1 mL of 10.0 M hydrazine (1.0 mmol) was added to the resulting suspensions under vigorous stirring. Immediately following the addition of hydrazine, the solution underwent a color change from transparent yellow to turbid orange. After 30 min of vigorous stirring, the solution mixture was centrifuged to remove large aggregates of NPs (4000 rpm, 3200*g* RCF_{avg}, 15 min), and then, the transparent reddish supernatant was dialyzed against deionized water using a dialysis membrane (MWCO 12000−14000, SpectraPore) for 3

dx.doi.org/10.1021/jp4027139 | J. Phys. Chem. C 2013, 117, 11686−11693

days to remove any byproducts and residuals. The prepared suspension of Au NPs exhibited a fairly good colloidal stability that lasted more than 6 months without any precipitation.

Reduction of Nitroarenes. To an aqueous solution of 7.50×10^{-4} M nitroarene (0.5 mol % with respect to the gold concentration), 0.566 mL of 6.63×10^{-5} M Au@DHBC NP catalyst was slowly added. To this mixture, 1.0 mL of 2.22 M $NaBH_4$ solution (300 equiv of substrate, 99%, Aldrich) was added until the deep yellow solution became colorless. The yellow color of the solution gradually vanished, indicating the reduction of 4-nitrophenol. The reaction progress was checked periodically by assessing a small portion of the reaction mixture at a regular time interval.

Characterizations. The morphology, size, and size distribution of the prepared Au NPs were investigated using transmission electron microscopy (TEM, JEOL JEM-2100, accelerating voltage of 200 kV, Gatan CCD camera). The absorbance of the Au NPs and the concentration of nitroarenes were characterized by using UV/vis spectroscopy (Shimadzu UV-1800). The concentration of Au NPs was measured using ICP-OES (720-ES, Varian). Thermogravimetric analysis (TGA) was conducted in air atmosphere at a heating rate of 10 °C/min using a thermogravimetric analyzer (Q200, TA Instrument). Fourier-transform infrared (FT-IR) spectra were obtained with a FT-IR spectrophotometer (Varian). Size distribution analysis was studied using dynamic light scattering (DLS, Nano ZS, Malvern, U.K., and BI-APD, Brookhaven Instrument, New York, USA).

RESULTS AND DISCUSSION

The synthesis of Au NPs using a DHBC as a template is illustrated in Scheme 1. Traditionally, DHBCs have been employed in the controlled growth of inorganic minerals, such as $CaCO_3$, $BaSO_4$, and $Ca_3(PO_4)_2$, with unusual structural complexity in aqueous solutions;[19,20] however, there are only a few examples of employing PEO-*b*-PAA DHBCs in the controlled synthesis of metal NPs.[18,21,22]

In our approach, we use the DHBC PEO-*b*-PAA as our template and stabilizer for Au NP synthesis. While the carboxylate group of the PAA block provides a site that can interact with metal precursors, the PEO block acts as a stabilizer for the controlled synthesis of Au NPs. Upon introducing a Au precursor ($HAuCl_4$) that preferentially interacts with the carboxylate of the PAA block by ligand exchange, the PAA blocks segregate to form micellar aggregates in solution. Although we have previously shown that Cu and RuO_2 NPs can be synthesized using a similar DHBC approach based on the electrostatic interactions between cationic metal ions (i.e., Cu^{2+} and Ru^{3+}) and the carboxylate group of PAA, it should be noted that the method presented in this study is somewhat counterintuitive because the Au precursor dissociates into anionic $AuCl_4^-$, which unlikely interacts with PAA through electrostatic interactions. Nevertheless, the selective interaction between the carboxylate (COO^-) group in the PAA block and the Au metal precursor can be carefully confirmed using FT-IR spectroscopy (Figure 1). Pure PEO-*b*-PAA shows a C═O stretching vibration of the carboxylic acid group at 1729 cm^{-1} and a C—O stretching vibration of the PAA block and the PEO block at 1242 and 1091 cm^{-1}, respectively (Figure 1a). Upon introduction of NaOH, the carboxylic acid groups of the PAA block deprotonate, as evidenced by the appearance of asymmetric and symmetric stretching vibration of the carboxylate (COO^-) groups in the PAA block at 1563 and

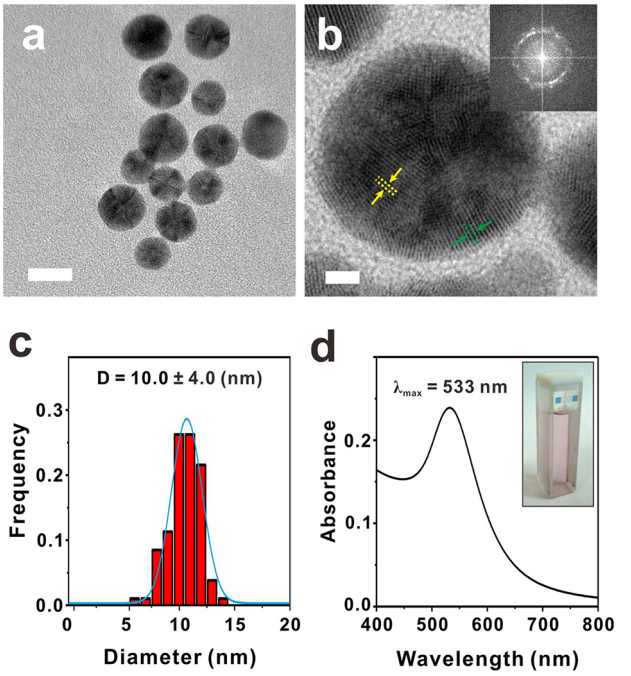

Figure 2. (a and b) TEM images of synthesized Au@DHBC. The scale bars in panels a and b represent 10 and 2 nm, respectively. The inset in part b shows the crystalline lattice fringes of 0.204 nm (yellow mark) and 0.236 nm (green mark), corresponding to the primary reflection of the (200) and (111) lattice of Au NP, respectively. (c) Corresponding size distribution histogram of as-prepared Au@DHBC NPs. (d) UV/vis spectrum of a synthesized suspension of Au@DHBC NPs. The inset shows the photograph image of a suspension of Au@DHBC NPs.

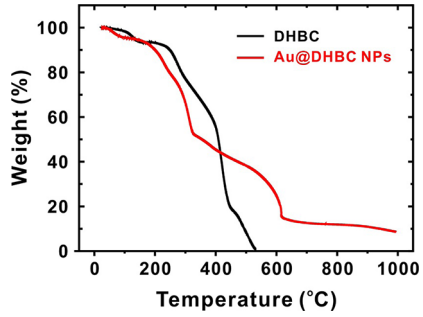

Figure 3. Thermogravimetric analysis (TGA) curves of (black) pure DHBC of PEO-*b*-PAA and (red) synthesized Au@DHBC NPs. The samples were subjected to heating at a rate of 10 °C min^{-1} under air atmosphere.

1429 cm^{-1}, respectively (Figure 1b). After the addition of the Au metal precursor, the peak at 1429 cm^{-1} is considerably diminished due to the strong coordinative complexation between the Au precursor and the carboxylate groups. A previous report has shown that carboxylate groups in citric acid can displace with the Cl^- ligand of $AuCl_4^-$ anions.[23] In addition, the disappearance of peaks observed in the carboxylate group was shown to indicate the formation of a Au(III)—O bond with the COO^- group of the PAA block,[24] which is in good agreement with our results.

The coordination modes formed between the metal precursor and the carboxylate groups of DHBC can be further confirmed by analyzing the FT-IR spectrum in Figure 1c. In general, the metal carboxylate coordination modes can be

dx.doi.org/10.1021/jp4027139 | J. Phys. Chem. C 2013, 117, 11686−11693

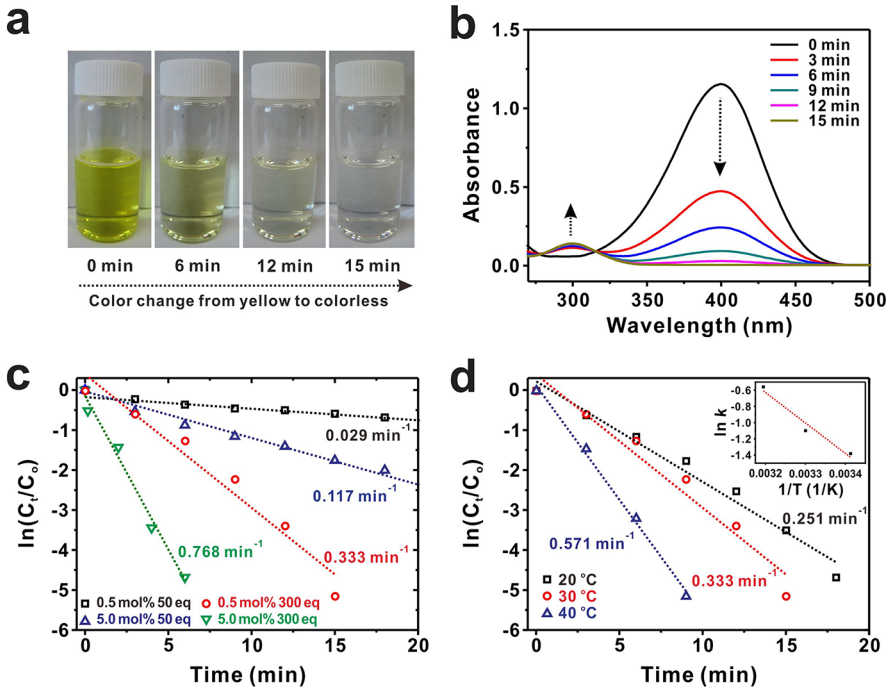

Figure 4. (a) The color change of 4-nitrophenol reduction with Au@DHBC NP catalyst and $NaBH_4$. (b) Representative time-dependent UV/vis absorption spectra for the reduction of 4-nitrophenol over Au@DHBC NP catalyst in aqueous media at 303 K. (c) Plot of $\ln(C_t/C_0)$ versus time spectra for the reduction of 4-nitrophenol over Au@DHBC catalyst under different mol % of catalyst and equivalents of $NaBH_4$ used. (d) Plot of $\ln(C_t/C_0)$ versus time for the reduction of 4-nitrophenol over Au@DHBC NP catalysts under different temperatures at 0.50 mol % catalyst and 300 equiv of $NaBH_4$. The inset shows the corresponding Arrhenius plot.

Table 1. Reduction of Various Nitroarenes Using Au@DHBC NP Catalyst[a]

Entry	Substrate	Product	Time[b]/min	TOF[c]/h^{-1}
1			15	800
2			10	1200
3			25	480
4			6	2000
5			3	4000
6			6	2000

[a]Reaction conditions: 10 mL of 7.50×10^{-4} M nitroarenes, 0.566 mL of 6.63×10^{-5} M Au@DHBC NP catalyst (0.50 mol % with respect to the Au concentration), 1.0 mL of 2.22 M $NaBH_4$ (300 equiv to the substrate). [b]Time was determined when over 99.9% of nitroarenes were reduced. [c]TOF is the ratio of the converted substrate to Au NPs catalyst used per unit time.

determined by the position and separation (Δ) of carboxylate bands in the 1300−1700 cm^{-1} range; for example, the unidentate mode (Δ > 200 cm^{-1}), bidentate mode (Δ > 110 cm^{-1}), and bridging mode (140 cm^{-1} < Δ < 200 cm^{-1}) can be identified by the separation between two characteristic bands of the carboxylate groups.[25,26] The separation (Δ) between the two carboxylate groups at 1563 and 1409 cm^{-1} in Figure 1c corresponds to the bridging mode. Additionally, the separation between the two carboxylate bands at 1563 and 1453 cm^{-1} can be assigned a bidentate coordination mode; however, it is not clearly discernible, as the peak at 1453 cm^{-1} is overlapped with a scissoring band of methylene group ($-CH_2-$) in the polymer. Therefore, the Au precursor can interact with the carboxylate group by a coordinative bond mainly with a bridging mode (Figure 1). Furthermore, the peak at 1099 cm^{-1} from the ether group (C−O−C) in the PEO block remains unchanged, suggesting that the preferential interaction between PAA and the metal precursor is dominant, as illustrated in Scheme 1. These selective coordinative interactions induce the DHBCs to form the micellar aggregates of approximately 4.4 nm in size, as determined by dynamic light scattering (DLS) (Figure S1, Supporting Information). In our previous reports, the triggered formation of micellar aggregates with a similar core−shell type structure was proposed with other metal ions such as Cu^{2+} and Ru^{3+} that formed complexes with DHBCs.[17,18]

Once their formation is induced, the PEO-*b*-PAA micelle acts as a nanoreactor to template the growth of a NP within the micellar core upon the addition of a reducing agent, N_2H_4. When N_2H_4 is added to the mixture to induce simultaneous nucleation and growth of NPs, the solution turns from transparent yellow to turbid red, signaling the formation of Au NPs within the DHBC template. Centrifuge cycles are performed immediately after reducing the Au precursor to remove unwanted aggregates as well as to obtain NPs with a

dx.doi.org/10.1021/jp4027139 | J. Phys. Chem. C 2013, 117, 11686−11693

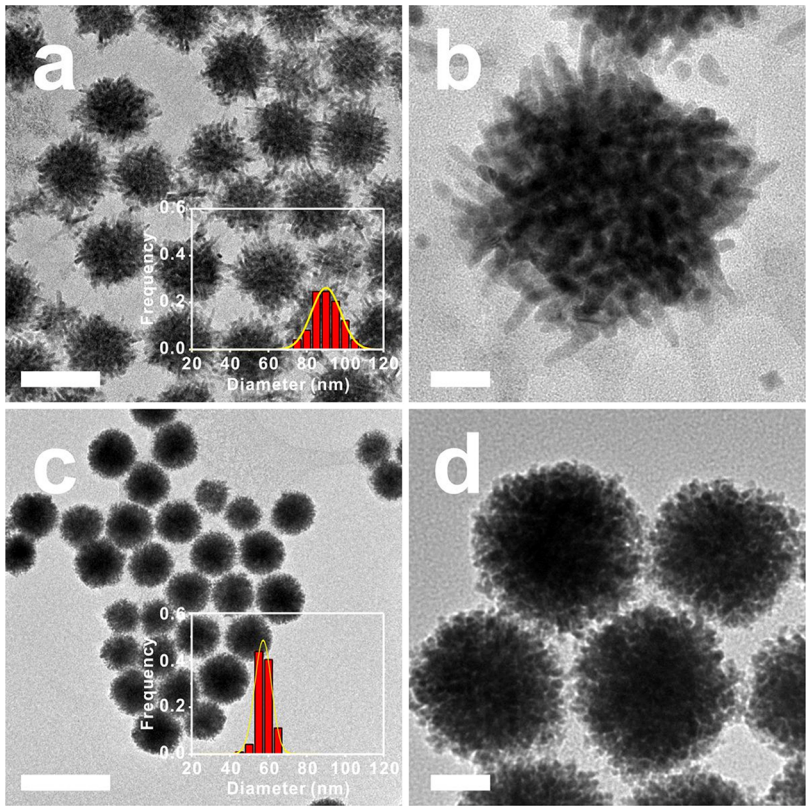

Figure 5. TEM images of the synthesized (a, b) Pd@DHBC NPs and (c, d) Pt@DHBC NPs with a histogram of size distribution. The average diameter is 87.9 ± 18.1 nm for Pd NPs and 55.5 ± 10.6 nm for Pt NPs, respectively. The scale bars in (a, c) and (b, d) represent 100 and 20 nm, respectively.

proper size distribution and an appropriate concentration. The prepared suspension of Au@DHBC NPs remains stable for several months without noticeable aggregation because the PEO block sterically stabilizes the NPs in aqueous solution (Figure 2d). The zeta-potential of Au@DHBC NPs is measured to be around −29 mV due to the presence of residual carboxylate groups in DHBCs. In clear contrast, a homopolymer of PAA with a similar molecular weight does not yield such a stable suspension of NPs, which highlights the important role of the PEO block in stabilizing the resulting Au NPs.[17]

The morphology and structure of the synthesized Au@DHBC NPs are characterized with transmission electron microscopy (TEM) and UV/vis spectroscopy (Figure 2). The TEM images of the synthesized Au NPs show a spherical morphology with an average diameter of 10.0 ± 4.0 nm averaged over 100 NPs after centrifuge to remove large aggregates (Figure S2, Supporting Information). High-resolution TEM in Figure 2b further reveals that Au NPs have a crystalline lattice fringe of 0.204 nm (yellow mark) and 0.236 nm (green mark), corresponding to the primary reflection of the (200) and (111) lattice of Au, respectively.

The characteristic surface plasmon resonance (SPR) peak of Au@DHBC NPs is also observed at 533 nm, which is slightly red-shifted when compared to that of other Au NPs with a similar diameter dispersed in an aqueous medium. In general, the Mie theory suggests that an increase in the refractive index of the medium red-shifts the SPR peak of Au NPs.[27] Thus, the red-shift likely originates from the high refractive index (n_{PAA} = 1.418) of the PAA block surrounding the Au@DHBC NPs (the refractive index of a typical aqueous solution, n_{H_2O} = 1.333), suggesting the formation of core−shell type Au NPs surrounded by the DHBC template. We note that, due to the low electron density of the DHBC, the presence of the PEO-*b*-PAA surrounding the Au NPs cannot be directly investigated under TEM. Thus, Au@DHBC NPs are analyzed using DLS to verify the existence of a thin PEO-*b*-PAA shell. The DLS measurement yields an average diameter of 13.97 nm, which is slightly larger than that observed under TEM, indicating the presence of a thin shell of DHBC surrounding the Au NPs (Figure S1, Supporting Information). We also investigate ways to control the size of Au NPs by varying the amount of Au precursor at a fixed concentration of DHBC, as well as varying the type of reductant (Figures S3 and S4, Supporting Information). The size of Au NPs is decreased by lowering the concentration of the Au precursor at a fixed polymer concentration, albeit with a relatively broad size distribution.

The thermal stability as well as the relative composition of the DHBC in the synthesized Au@DHBC NPs is estimated on the basis of the thermogravimetric analysis (TGA) (Figure 3). As shown in the TGA curve of Au@DHBC NPs, an initial mass loss of water at around 57.8 °C is observed. Following the initial loss of water, the second precipitous drop in mass begins at around 230 °C, which is associated with the degradation of the DHBCs. Characteristic peaks in the range 230−613 °C are observed in the differential TGA curve, which can be attributed to the degradation of PEO-*b*-PAA. Interestingly, in accord with the FT-IR data, TGA also indicates that the specific interactions between the polymer and the metal precursor increase the degradation temperature of the DHBCs from 530 to 613 °C. Finally, the subsequent weight loss corresponds to the conversion of the residual DHBCs into an amorphous

dx.doi.org/10.1021/jp4027139 | J. Phys. Chem. C 2013, 117, 11686−11693

carbonaceous layer around Au NPs, of which mass fraction is deduced to be approximately 16% of Au NPs present within the DHBC template. From the combination of TGA and TEM data, we calculate that approximately 2.73×10^3 mol of PEO-*b*-PAA chains remain per each Au NP. Furthermore, a residual polymeric layer is found around the aggregated Au NPs after thermal treatment (Figure S5, Supporting Information).

We test the utility of Au@DHBC NPs in the catalytic reduction of a series of nitroarenes. Nitroarenes are a class of toxic and poisonous chemicals; as such, there have been active efforts to develop methods to decompose nitroarenes, including physical, biological, and chemical techniques.[28] In particular, catalytic reduction of nitroarenes using various nanostructured materials has been demonstrated with its synthetic utility and mild reaction conditions. For example, hollow Au nanostructures, bimetallic Pt and Pd, and hybrid NPs on a support have been demonstrated to be effective in the reduction of nitroarenes.[29−33]

In order to evaluate the efficiency of the Au@DHBC NP as a catalyst, we first employ the reduction of 4-nitrophenol to 4-aminophenol in the presence of a hydrogen source, $NaBH_4$ (Figure 4). Initially, the 4-nitrophenol solution has a light yellow color, which turns dark yellow upon the addition of $NaBH_4$ due to the formation of 4-nitrophenolate (Figure S6, Supporting Information). However, with the use of Au@DHBC NPs, the dark yellow color gradually fades away with the progression of the reduction to 4-aminophenol. The kinetics of the reaction can be periodically monitored using UV/vis spectroscopy measurements. Specifically, the absorption of 4-nitrophenol at 400 nm rapidly decreases with a concomitant increase in the peak at 300 nm, which can be attributed to the production of 4-aminophenol (Figure 4b). The isosbestic point between the two peaks is also observed, suggesting that the two principal species are responsible for the conversion reaction. On the basis of the UV/vis spectra, therefore, the pseudo-first-order reaction kinetics is applied to determine the reaction rate constant, *k*, for the reaction. We also conduct several control experiments to determine the optimum reaction condition of the Au@DHBC NP catalyst. In addition, we vary the concentration of catalyst and reductant while keeping the reaction temperature constant. From the linear relations of $\ln(C_t/C_o)$ with time, we find the rate constant, *k*, at 30 °C to be 0.029, 0.117, 0.333, and 0.768 min^{-1} with different concentrations of catalyst and reductant (Figure 4c). These results are all comparable or superior to those reported previously, which are in the range 10^{-1}−10^{-3} min^{-1} under similar reaction conditions, indicating a high catalytic activity of Au@DHBC NP prepared with the DHBC template.[34] In terms of turnover frequency (TOF), which correlates the degree of reaction per unit time with the amount of catalyst used during the reaction, the 0.5 mol % Au NPs with 300 equiv of $NaBH_4$ yielded the optimal catalytic activity among all samples tested. Interestingly, it is noted that Au NP catalyst with the DHBC shell (TOF of 800 h^{-1}) displays a superior catalytic activity in the reduction of 4-nitrophenol to that of Au NPs prepared by citrate reduction (TOF of 570 h^{-1}) with a similar diameter of 10.7 ± 4.3 nm (Figure S7, Supporting Information). This observation suggests that not only the core Au NPs but also the surrounding DHBCs are playing a critical role in the enhancement of the reaction efficiency. In concert with our observation, Crooks and co-workers have previously observed enhanced catalytic activity of metal NPs synthesized within dendrimer templates.[35−37] They attributed that the dendrimer encapsulated NPs could exhibit an enhanced catalytic efficiency due to the confinement effect within the sterically confined dendrimer core. In addition, it was presented that dendrimer could serve as a selective gate to permit small molecule reactants to be located near the catalytic NPs for efficient reaction.[38] When compared to other reports which used amphiphilic block copolymers to make Au NPs, the Au@DHBC NPs exhibit a greater catalytic activity. This value is comparable to the recent study by Chen and co-workers, which showed that Au catalysts coated with an amphiphilic block copolymer, polystyrene-*block*-poly(4-vinyl pyridine) (PS-*b*-P4VP), results in a TOF value of 443 h^{-1} in 4-nitrophenol reduction.[39] Moreover, the catalytic activity of Au@DHBC NP is comparable to the catalytic activity of hybrid composites such as Au-graphene, which was previously reported by our group, demonstrating a TOF value of 400 h^{-1}, or Au-carbon nanotube, investigated by Li and co-workers, reporting a TOF value of 35 h^{-1} of TOF in 4-nitrophenol reduction. Both graphene and carbon nanotube are used as a support to increase the efficiency and stability of catalysts; thus, highlighting the excellence of Au@DHBC NP as a catalyst.[29,30] In another example, Jin et al. recently reported the synthesis of Au NPs loaded TiO_2 microspheres and their application as a catalyst for 4-NP reduction with a high catalytic efficiency with a TOF value of 4800 h^{-1}.[40]

The reduction of 4-nitrophenol to 4-aminophenol is known to be thermodynamically favorable with a standard reduction potential of −0.76 V with a use of hydrogen source of $NaBH_4$ that possesses the reduction potential of −1.33 V. 4-Nitrophenol nevertheless does not spontaneously reduce due to the high activation energy of this reaction. In agreement with this argument, we find that the peak at 400 nm indicating the concentration of 4-nitrophenol does not change for days without a catalyst (Figure S8, Supporting Information). We also find that the reaction rate is quite sensitive to temperature. Thus, by carrying out the identical reaction at different temperatures, the activation energy of the reaction is determined to be 31.2 kJ mol^{-1} according to the Arrhenius plot (Figure 4d).

We further investigate the catalytic activity of Au@DHBC NPs for the reduction of a series of other nitroarene derivatives (Table 1). Here, we choose to run the reactions in the optimized condition of 0.5 mol % catalyst with 300 equiv of $NaBH_4$ to clearly monitor the conversion efficiency of the reaction. As shown in Table 1, we find that our Au@DHBC NPs exhibit high reactivity with excellent yields toward a series of model nitroaniline and nitrophenol compounds regardless of the types and position of the substituents. Interestingly, when the reduction of 4-, 3-, and 2-nitrophenols (or nitroanilines) is catalyzed by Au@DHBC NPs, the 3-nitrophenol (or nitroaniline) shows a better catalytic activity than 4- or 2-nitrophenols (or nitroanilines) due to the charge stabilization of anionic intermediates formed during the course of the reaction. For example, the remarkable TOF in entry 5 is as high as 4000 h^{-1}, calculated on the basis of moles of nitroarene converted per mole of the Au NP catalyst per 1 h under the present reaction conditions.

Finally, in order to demonstrate the versatility of the DHBC-based approach, we synthesize other metal NPs such as Pd and Pt, based on the identical protocol described for Au@DHBC NPs. As presented in Figure 5, highly water-dispersible Pd@DHBC and Pt@DHBC NPs are successfully prepared with a controllable size (see the Supporting Information for details). It

dx.doi.org/10.1021/jp4027139 | J. Phys. Chem. C 2013, 117, 11686−11693

is also interesting to note that the morphology of these NPs is significantly different from the spherical Au@DHBC NPs. This result further highlights the potential of our DHBC-based approach as a facile and general means of producing metal nanostructures with different functionalities for various applications, which will be the subject of our ongoing endeavor.

CONCLUSION

We have developed a simple, facile method of synthesizing gold nanoparticles (Au NPs) using a double hydrophilic block copolymer (DHBC), PEO-*b*-PAA, as a soft template through the coordinative interactions between the carboxylate groups of the PAA block of the polymer and the Au precursor. Each segment of the DHBC plays an important role in forming stable Au NPs; the PAA block of the DHBC interacts with the Au precursor to form micelle aggregates and template Au NPs, whereas the PEO block stabilizes the NPs in aqueous solution. The synthesized Au@DHBC NPs are successfully employed in the catalytic reduction of a series of nitroarenes with an efficient catalytic activity by the confined interior of the polymeric shell around the Au NPs, further highlighting the importance of the DHBC template. We anticipate that Au NPs synthesized with DHBCs will broaden the application of Au NPs as heterogeneous catalysts in aqueous solutions. Moreover, the approach of synthesizing metal NPs with DHBCs can lead to a facile and general means of producing metal nanostructures with different functionalities for various applications.

ASSOCIATED CONTENT

Supporting Information

Synthetic protocol for all NPs prepared in this study, DLS analysis, additional TEM images, and UV/vis spectra of control experiments. This material is available free of charge via the Internet at http://pubs.acs.org.

AUTHOR INFORMATION

Corresponding Author

*Phone: +82-52-217-2923. E-mail: bskim19@unist.ac.kr.

Notes

The authors declare no competing financial interest.

ACKNOWLEDGMENTS

This research was supported by the New & Renewable Energy of the Korea Institute of Energy Technology Evaluation and Planning (KETEP) grant funded by the Korea government Ministry of Knowledge Economy (20113020030060) and the National Research Foundation of Korea (NRF) funded by the Ministry of Education, Science and Technology (2010-0029434, 2011-0015061). This work was also supported by the 2009 Research Fund (1.090048.01) of UNIST (Ulsan National Institute of Science and Technology). J.K. and D.L. acknowledge the support of an NSF CAREER Award (DMR-1055594).

REFERENCES

(1) Skrabalak, S. E.; Chen, J.; Sun, Y.; Lu, X.; Au, L.; Cobley, C. M.; Xia, Y. Gold Nanocages: Synthesis, Properties, and Applications. *Acc. Chem. Res.* **2008**, *41*, 1587−1595.

(2) Corma, A.; Garcia, H. Supported Gold Nanoparticles as Catalysts for Organic Reactions. *Chem. Soc. Rev.* **2008**, *37*, 2096−2126.

(3) Grzelczak, M.; Pérez-Juste, J.; Mulvaney, P.; Liz-Marzán, L. M. Shape Control in Gold Nanoparticle Synthesis. *Chem. Soc. Rev.* **2008**, *37*, 1783−1791.

(4) Daniel, M. C.; Astruc, D. Gold Nanoparticles: Assembly, Supramolecular Chemistry, Quantum-Size-Related Properties, and Applications toward Biology, Catalysis, and Nanotechnology. *Chem. Rev.* **2004**, *104*, 293.

(5) Hu, M.; Chen, J.; Li, Z. Y.; Au, L.; Hartland, G. V.; Li, X.; Marquez, M.; Xia, Y. Gold Nanostructures: Engineering Their Plasmonic Properties for Biomedical Applications. *Chem. Soc. Rev.* **2006**, *35*, 1084−1094.

(6) Turkevich, J.; Stevenson, P. C.; Hillier, J. A Study of the Nucleation and Growth Processes in the Synthesis of Colloidal Gold. *Discuss. Faraday Soc.* **1951**, *11*, 55−75.

(7) Frens, G. Controlled Nucleation for the Regulation of the Particle Size in Monodisperse Gold Suspensions. *Nature* **1973**, *241*, 20−22.

(8) Brust, M.; Walker, M.; Bethell, D.; Schiffrin, D. J.; Whyman, R. Synthesis of Thiol-Derivatised Gold Nanoparticles in a Two-Phase Liquid−Liquid System. *J. Chem. Soc., Chem. Commun.* **1994**, 801−802.

(9) Busbee, B. D.; Obare, S. O.; Murphy, C. J. An Improved Synthesis of High-Aspect-Ratio Gold Nanorods. *Adv. Mater.* **2003**, *15*, 414−416.

(10) Jana, N. R.; Gearheart, L.; Murphy, C. J. Seeding Growth for Size Control of 5−40 nm Diameter Gold Nanoparticles. *Langmuir* **2001**, *17*, 6782−6786.

(11) Sohn, B. H.; Choi, J. M.; Yoo, S. I.; Yun, S. H.; Zin, W. C.; Jung, J. C.; Kanehara, M.; Hirata, T.; Teranishi, T. Directed Self-Assembly of Two Kinds of Nanoparticles Utilizing Monolayer Films of Diblock Copolymer Micelles. *J. Am. Chem. Soc.* **2003**, *125*, 6368−6369.

(12) Mössmer, S.; Spatz, J. P.; Möller, M.; Aberle, T.; Schmidt, J.; Burchard, W. Solution Behavior of Poly(styrene)-block-poly(2-vinylpyridine) Micelles Containing Gold Nanoparticles. *Macromolecules* **2000**, *33*, 4791−4798.

(13) Maye, M. M.; Chun, S. C.; Han, L.; Rabinovich, D.; Zhong, C. J. Novel Spherical Assembly of Gold Nanoparticles Mediated by a Tetradentate Thioether. *J. Am. Chem. Soc.* **2002**, *124*, 4958−4959.

(14) Teranishi, T.; Hasegawa, S.; Shimizu, T.; Miyake, M. Heat-Induced Size Evolution of Gold Nanoparticles in the Solid State. *Adv. Mater.* **2001**, *13*, 1699.

(15) Jana, N. R.; Gearheart, L.; Murphy, C. J. Evidence for Seed-Mediated Nucleation in the Chemical Reduction of Gold Salts to Gold Nanoparticles. *Chem. Mater.* **2001**, *13*, 2313−2322.

(16) Ji, X.; Song, X.; Li, J.; Bai, Y.; Yang, W.; Peng, X. Size Control of Gold Nanocrystals in Citrate Reduction: the Third Role of Citrate. *J. Am. Chem. Soc.* **2007**, *129*, 13939−13948.

(17) Seo, E.; Lee, T.; Lee, K. T.; Song, H. K.; Kim, B. S. Versatile Double Hydrophilic Block Copolymers: Dual Role as Synthetic Nanoreactor and Ionic and Electronic Conducting Layer for Ruthenium Oxide Nanoparticle Supercapacitors. *J. Mater. Chem.* **2012**, *22*, 11598−11604.

(18) Kim, A.; Sharma, B.; Kim, B. S.; Park, K. H. Double-Hydrophilic Block Copolymer Nanoreactor for the Synthesis of Copper Nanoparticles and for Application in Click Chemistry. *J. Nanosci. Nanotechnol.* **2011**, *11*, 6162−6166.

(19) Nakashima, K.; Bahadur, P. Aggregation of Water-Soluble Block Copolymers in Aqueous Solutions: Recent Trends. *Adv. Colloid Interface Sci.* **2006**, *123*, 75−96.

(20) Cölfen, H. Double-Hydrophilic Block Copolymers: Synthesis and Application as Novel Surfactants and Crystal Growth Modifiers. *Macromol. Rapid Commun.* **2001**, *22*, 219−252.

(21) Taubert, A.; Palms, D.; Weiss, Ö.; Piccini, M. T.; Batchelder, D. N. Polymer-Assisted Control of Particle Morphology and Particle Size of Zinc Oxide Precipitated from Aqueous Solution. *Chem. Mater.* **2002**, *14*, 2594−2601.

(22) Qi, L.; Cölfen, H.; Antonietti, M. Synthesis and Characterization of CdS Nanoparticles Stabilized by Double-Hydrophilic Block Copolymers. *Nano Lett.* **2001**, *1*, 61−65.

(23) Ojea-Jiménez, I.; Romero, F. M.; Bastús, N. G.; Puntes, V. Small Gold Nanoparticles Synthesized with Sodium Citrate and Heavy Water: Insights into the Reaction Mechanism. *J. Phys. Chem. C* **2010**, *114*, 1800−1804.

(24) Ivanova, B. B. Solid-State Linear-Dichroic Infrared Spectroscopic Analysis of the Dipeptide S-Phe−S-Phe and Its Mononuclear Au(III) Complex. *J. Coord. Chem.* **2005**, *58*, 587−593.
(25) Lu, Y.; Miller, J. D. Carboxyl Stretching Vibrations of Spontaneously Adsorbed and LB-Transferred Calcium Carboxylates as Determined by FTIR Internal Reflection Spectroscopy. *J. Colloid Interface Sci.* **2002**, *256*, 41−52.
(26) Bronstein, L. M.; Huang, X.; Retrum, J.; Schmucker, A.; Pink, M.; Stein, B. D.; Dragnea, B. Influence of Iron Oleate Complex Structure on Iron Oxide Nanoparticle Formation. *Chem. Mater.* **2007**, *19*, 3624−3632.
(27) Chen, H.; Kou, X.; Yang, Z.; Ni, W.; Wang, J. Shape- and Size-Dependent Refractive Index Sensitivity of Gold Nanoparticles. *Langmuir* **2008**, *24*, 5233−5237.
(28) Vaidya, M. J.; Kulkarni, S. M.; Chaudhari, R. V. Synthesis of p-Aminophenol by Catalytic Hydrogenation of p-Nitrophenol. *Org. Process Res. Dev.* **2003**, *7*, 202−208.
(29) Li, H.; Jo, J. K.; Zhang, L.; Ha, C. S.; Suh, H.; Kim, I. A General and Efficient Route to Fabricate Carbon Nanotube-Metal Nanoparticles and Carbon Nanotube-Inorganic Oxides Hybrids. *Adv. Funct. Mater.* **2010**, *20*, 3864−3873.
(30) Choi, Y.; Bae, H. S.; Seo, E.; Jang, S.; Park, K. H.; Kim, B. S. Hybrid Gold Nanoparticle-Reduced Graphene Oxide Nanosheets as Active Catalysts for Highly Efficient Reduction of Nitroarenes. *J. Mater. Chem.* **2011**, *21*, 15431−15436.
(31) Lin, F.; Doong, R. Bifunctional Au−Fe3O4 Heterostructures for Magnetically Recyclable Catalysis of Nitrophenol Reduction. *J. Phys. Chem. C* **2011**, *115*, 6591−6598.
(32) Mahmoud, M.; Saira, F.; El-Sayed, M. Experimental Evidence for the Nanocage Effect in Catalysis with Hollow Nanoparticles. *Nano Lett.* **2010**, *10*, 3764−3769.
(33) Zeng, J.; Zhang, Q.; Chen, J.; Xia, Y. A Comparison Study of the Catalytic Properties of Au-Based Nanocages, Nanoboxes, and Nanoparticles. *Nano Lett.* **2009**, *10*, 30−35.
(34) Lee, J.; Park, J. C.; Song, H. A Nanoreactor Framework of a Au@SiO2 Yolk/Shell Structure for Catalytic Reduction of p-Nitrophenol. *Adv. Mater.* **2008**, *20*, 1523−1528.
(35) Crooks, R. M.; Zhao, M. Dendrimer-Encapsulated Pt Nanoparticles: Synthesis, Characterization, and Applications to Catalysis. *Adv. Mater.* **1999**, *11*, 217−220.
(36) Zhao, M.; Crooks, R. M. Homogeneous Hydrogenation Catalysis with Monodisperse, Dendrimer-Encapsulated Pd and Pt Nanoparticles. *Angew. Chem., Int. Ed.* **1999**, *38*, 364−366.
(37) Yeung, L. K.; Crooks, R. M. Heck Heterocoupling within a Dendritic Nanoreactor. *Nano Lett.* **2001**, *1*, 14−17.
(38) Crooks, R. M.; Zhao, M.; Sun, L.; Chechik, V.; Yeung, L. K. Dendrimer-Encapsulated Metal Nanoparticles: Synthesis, Characterization, and Applications to Catalysis. *Acc. Chem. Res.* **2001**, *34*, 181−190.
(39) Chen, X.; Zhao, D.; An, Y.; Zhang, Y.; Cheng, J.; Wang, B.; Shi, L. Formation and Catalytic Activity of Spherical Composites with Surfaces Coated with Gold Nanoparticles. *J. Colloid Interface Sci.* **2008**, *322*, 414−420.
(40) Jin, Z.; Xiao, M.; Bao, Z.; Wang, P.; Wang, J. A General Approach to Mesoporous Metal Oxide Microspheres Loaded with Noble Metal Nanoparticles. *Angew. Chem., Int. Ed.* **2012**, *51*, 6406−6410.